

Influence of Corrosion Rate on the Double Butt Welding Shapes Design for Low Carbon Steel

Dr. Hani Aziz Ameen*, Khairia Salman Hassan**
& Walid Khalid Abdul Kader***

Received on: 30/11/2010

Accepted on: 7/4/2011

Abstract

The aim of this paper is to demonstrate the influence of butt welding shapes on the corrosion rate, microstructure and temperature of carbon steel type St37. The double butt welding was performed by V angles 15° , 30° and 45° . The finite element analysis via ANSYS software is performed, this analysis includes a finite element model for the thermal welding simulation. The temperature distribution was obtained. From the results of the microscopic structure it is evident that the geometric shape has an important role in the welding process, when the geometric value of the welding region gets bigger, the faults get less due to increase of heat quantity in the welding region and the corrosion rate for the rain water is less than of sea water. The work presents the finite element model for numerical simulation of welding in carbon steel St37 double butt welding.

Keywords: Welding Technology , Finite Element Method, Heat Transfer, ANSYS software , Corrosion

تأثير معدل التآكل على تصميم وصلة اللحام التناكبي المزدوجة للفولاذ المنخفض الكربون

الخلاصة

في هذا البحث تم دراسة تأثير معدل التآكل وبحالتين ماء البحر وماء المطر على وصلة اللحام التناكبي المزدوجة، وتم دراسة البنية المجهرية وتوزيع درجات الحرارة لفولاذ كربوني نوع St37 حيث تم اللحام على وصلات تناكبية مزدوجة اجريت لها عملية تحضير بالزوايا $(15^\circ, 30^\circ, 45^\circ)$ V. تم استخدام طريقة العناصر المحددة من خلال برنامج ANSYS لتحليل عملية اللحام، وهذا التحليل تضمن التحليل الحراري لمنطقة اللحام. وقد تم استنتاج ان شكل منطقة اللحام لها تأثير كبير على البنية المجهرية لمنطقة اللحام حيث كلما كبرت منطقة اللحام فان العيوب سوف تقل بسبب زيادة كمية الحرارة في منطقة اللحام وايضا ان معدل التآكل في ماء المطر اقل من ماء البحر. تضمن البحث تحليل منطقة اللحام باستخدام طريقة العناصر المحددة واعداد نمذجة عديدة لعملية اللحام التناكبي المزدوج لفولاذ نوع St37.

Introduction

The butt welding is a process that is being widely used in industry for sheet joining purposes. Many applications of welding made of carbon steel (e.g. bridge structure, fuel tanks ..etc) are subjected to various

stresses (tensile, compressive, bending ..etc). The toughness and resistance of the welded piece to failure depending on many factors such as shape, design of the welding piece, the method implemented for welding and the nature of the applied stresses. Also

* College of Technical /Baghdad

** Institute of Technology /Baghdad

*** Materials Engineering Department, University of Technology / Baghdad

butt-welding is widely used in automotive industries to assemble various products. It is well known that the welding process relies on an intensely localized heat input, which tends to generate undesired residual stresses and deformations in welded structures, especially in the case of thin plates [1]. Therefore, estimating the magnitude of welding deformations and characterizing the effects of the welding conditions are deemed necessary. With modern computing facilities, the finite element technique has become an effective method for prediction and assessment of welding stresses [2]. Therefore, rapidly and accurately predicting welding induced distortion for real engineering applications is more challenging. Hani [3] (1998) explains the thermo-mechanical model which was developed using FE method to calculate temperature, stresses and distortions during elasto-plastic analysis. Linderger et al [4] (2002) presented a thermo-mechanical analysis in butt welding of copper canister for spent nuclear fuel. Anas and Abid [5] (2004) studied the finite element volume for modeling welds and it depicts a brief history of the simulation of welds. Dragi and Ivana [6] (2009) studied the finite element analysis of residual stresses in butt welding of two similar plates. Hani and Khairyria [7] (2010) studied experimentally and numerically the influence of single butt welding shapes design on the microstructure and stresses of low carbon steel. This paper describes the corrosion rate in the double butt welding and microscopic structure of welded region and the modeling of the welding process using the finite element modeling technique, three dimensional thermo-mechanical model will be used to model this process.

Experimental

Choice of Metals

Low carbon steel St37 was chosen according to the Russian Standards (Gost). Its chemical analysis is shown in Table (1) and its done in the Institute of Technology/ Baghdad.

Preparation of welding piece

- Selection metallic plates, 10 mm thick, 60 mm long and 40 mm wide .
- making preparation double V angle of 15°.
- The operation is repeated on the remaining pieces to make V angles of (30° and 45°)

Welding Process

Welding is done by electric arc (MIG) on the piece. The conditions for the process are indicated in Table(2) .

The Input heat quantity is calculated by the following equation[1]:

$$\text{Heat Input} = \frac{543 \times I \times V \times 60}{S} \dots (1)$$

where

I Current (ampere) , V.... Voltage (Volt) and S...Welding speed (m/min).

After the welding process, the welded pieces were tested by X-ray radiography. Faulty pieces were excluded. Pieces without faults were prepared in the following manner :

Grinding the specimens by sandpapers of grades 220, 400, 800, and 1100 granule/cm² (mesh), then polishing process by using of polishing cloth with Aluminum oxide (Al₂O₃, having particles of 5 micron) as a polishing assistant, after that etching by Nital solution , which is composed of (98% Methyl alcohol + 2% Nitric acid) is done. Finally examination of the microstructure by a light microscope of 400X magnification and photographing the microstructure .

Fig.(1) shows the microstructure for base metal, Heat affected zone (Haz) and welded zone.

Welding Wire

The welding wire (AWS ER705-6) is used with 1.2mm diameter in which the chemical composition is shown in Table(3), its done in the Institute of Technology/ Baghdad.

Corrosion Test

1-Classification of specimens

After preparation, the specimens were classified for two groups as shown below.

A	Specimen immersed in sea water
B	Specimen immersed in rain water

2- Preparation the water solution

The water solution is prepared , which is consists of :

- 1- Sea water of 35 gram of sodium chloride with 1000 gram of distil water . The pH of the solution is measured by pH meter and its found 6.9 .
- 2- Rain water , it is collected after falling the three rain and pH is measured and it is found 4.

3- Electrochemical Tests

The prepared specimen was fixed in the holder shown in Fig.(2). The reference electrode was fixed about (1 mm) apart from the surface of the specimen to be tested. The reference electrode used in this study was saturated calomel electrode (SCE). The auxiliary electrode used in the electrochemical cell was platinum type. The specimen holder (working electrode), together with the reference and auxiliary electrode were inserted in their respective positions in the electrochemical cell used for this purpose that can fit all these electrodes as shown in Fig.(3). The cell used was made of glass.

Constant potentials (anodic or cathodic) can be imposed on the

specimen, by using the potentiostat (Mlab200 of Bank Eleck .Germany). This potentiostat is able to induce a constant potentials ranging from (± 1 Iv) the potentials of the standard reference electrode used in this study (SCE).

The potential difference between the working and the reference electrode (WE - RE)and any current passing in the circuit of working electrode were the auxiliary electrode can be measured by using the SCI computer software. Any potential difference between the working and reference electrodes and also any current in the working electrode circuit can be automatically recorded. The results and plots were recorded using window XP. The scan rate can be selected also.

Polarization resistance tests were used to obtain the micro cell corrosion rates. In the tests, cell current reading was taken during a short, slow sweep of the potential. The sweep was taken from (-100 to +100) mv relative to (OPC)[8,9]. Scan rate defines the speed of potential sweep in mv /sec. In this range the current density versus voltage curve is almost nearly linear. A linear data fitting of the standard model gives an estimate of the polarization resistance, which used to calculate the corrosion current density (I_{corr}) and corrosion rate. The tests were performed by using a WENKING MLab multi channels and SCI-Mlab corrosion measuring system from Bank Electronics- Intelligent controls GmbH, Germany 2007, as shown in Fig.(4).

Theoretical Consideration

Theoretically the welding process can be considered either using a thermal or a mechanical analysis. Thermal stresses induced during a welding process are obtained from the temperature distributions determined by the thermal model. The stresses from each temperature increment are

added to the nodal point location to determine the updated behavior of the model before the next temperature increment. There are two distinct methods: sequential and direct in a coupled-field analysis. Which procedure for a coupled-field analysis will be used depends on which fields are being coupled. The sequential method involves two or more sequential analyses that belong to a different file. Adversely, the direct method usually involves just one analysis that uses a coupled-field element type containing all necessary degrees of freedom. In this work, the process of welding is simulated by the finite element method. The welding process computation can be done to get thermal and mechanical analysis, the temperatures are determined as a function of time in the analysis. Then, the mechanical analysis employs the previous results to get displacements at nodes and stresses at integration points. Since the thermal field has a strong influence on the stress field with little inverse influence. Moreover, a three dimensional finite element analysis is the optimum method of ascertaining the thermal cycle of welding. Therefore, in this paper, the welding process is simulated using a direct coupled three dimensional thermo-mechanical finite element formulation based on the ANSYS code[10]. For both the thermal and mechanical analysis, temperature-dependent thermo-physical and mechanical properties of materials are incorporated. The temperature dependent thermal material properties for the plates, heat affected zone and the filler weld material were assumed to be the same. The plasticity material model used was von Mises rate-independent kinematic bilinear hardening. Table(4) illustrated the material properties[6]. Fig.(5) shown

the element type SOLID98 which has coupled degree of freedom was used for the thermal- mechanical analysis in the present work. Fig.(6) shows the model in ANSYS program. The ANSYS steps can be demonstrated in the following program which is done in ANSYS to make the butt welding analysis[11].

```

/view,1,1,1,1
/prep7
et,1,solid87
mp,kxx,1,44.5
mp,dens,1,7.85
mp,c,1,0.475
x1=0.003 : y1=0.002: theta=45
*afun,deg
xx=(0.01-(0.005+y1/2))*tan(theta)
k,1,0,0
k,2,0.06-xx,0
k,3,0.06,(0.01-(0.005+y1/2))
k,4,0.06,(0.01-(0.005+y1/2))+y1
k,5,0.06-xx,0.01
k,6,0,0.01
l,1,2 :1,2,3: 1,3,4:1,4,5
l,5,6:1,6,1: k,7,0.06+x1+xx,0
k,8,0.06+x1,(0.01-(0.005+y1/2))
k,9,0.06+x1,(0.01-(0.005+y1/2))+y1
k,10,0.06+x1+xx,0.01
k,11,0.06+x1+0.06,0.01
k,12,0.06+x1+0.06,0
l,7,8 : 1,8,9: 1,9,10: 1,10,11
l,11,12 : 1,12,7
k,13,0.06+(x1/2),0.0125
spline,5,13,10
k,14,0.06+(x1/2),-0.0025
spline,2,14,7: csys,1
a,1,2,3,4,5,6: a,2,14,7,8,3
a,3,8,9,4: a,9,10,13,5,4
a,7,8,9,10,11,12
voffst,1,0.04:voffst,2,0.04
voffst,3,0.04:voffst,4,0.04
voffst,5,-0.04:vglue,all
vmesh,all
finish
/solu
antype,trans
asel,s,area,,12 :asel,a,,,35
nsla,s:d,all,all:allsel

```

asel,s,,26:asel,a,,44
 nsla,s:tunif,25
 q=34603792.94
 sf,all,hflux,q
 allsel:time,75:deltim,3
 autots,on:outres,,all:outpr,,all
 cnvtol,temp,20,0.01
 solve
 finish

Results and Discussion

By observing the photos of the microstructure and calculated heat quantity as shown in Table(2), it is found that with decreasing preparation angle of the welded plates, the heat quantity increases, quantity of welding metal decreases, welding region possesses better quantities, greater heat transfer to adjoining region (which is effected directly by heat), while it can be shown that the heat quantity is equal with 30° V and 45° V due to the same input parameters. Increasing of heat quantity contributes at growth of granules' volume with high ductility due to slow cooling of the metal during welding as well as weak mechanical properties (resistance to tension and hardness). Therefore, it is preferred that the welding angle be 45° for homogenous heat distribution to it. Fig.(6) shows the variance of the particles of the weld region for the different geometry of 15° double V, 30° double V, 45° double V as follows:-

It is evidenced from the figure that the microstructure becomes finer with the increase of the geometric form's value of the welding region for specimens 15°, 30°, 45° respectively. Fig.(7) shows the temperature distribution in the weld region. Weldability differs from one metal or alloy to another. It depends on its material properties as shown in Table(4). To insure good weld for the metal, the latter should be a good heat conductor, of little shrinkage and of

small longitudinal expansion index. Poor heat conductivity leads to heat concentration in small part and non equality of the temperature of the whole work. The more intense are the generated internal stresses, the greater would be the longitudinal expansion index and its shrinkage is greater. Fig.(8) is a schematic drawing [7] of a cross-section of the weld and its adjoining region in which is manifested the thermal influence of the weld. The weld structure consists of region "a" of large sized cast structure which is a characteristic of the alloyed metal. This region is followed by the region of excess heating "b"; this is due to influence of high temperature excess heating greatly lowers the plasticity and shock resistance. It forms in the region "c" which is heated to a little higher temperature than line GS (i.e. line between two regions in Fig.(8)) upon air cooling. Gradually, this region shifts to region "d" which is heated to a temperature below line GS. Upon slow cooling, this leads to incomplete plasticizing. In region "e" the temperature of the heated metal does not reach to the region of phase recrystallization of the steel. Thus, the structure of the base metal in it is not influenced by the heating due to welding. So, the weld creates different structure in the adjoining its regions causing great degradation of its properties. Shifts in the structures of regions "a", "b" and "c" help at generation of internal stresses in it. Evidently good welding quality would be better as the region adjacent to the seams of the weld is smaller. Weldability of low carbon steel down to 0.2% is very good. By increasing the carbon percentage, heat conductivity of steel decreases and the internal stresses in it are increased.

Fig.(9) shows the Tafel and cyclic polarization curve of low carbon steel

in sea and rain water and Table(5) shows the current density. The current density (as shown from these Figures and Tables) decreases sharply when the using rain water.

Conclusions

1. Weld angle depends on the thickness of the metal to be welded.
2. When the welding angle is increased, the stuffing material and its properties, have an influence on the properties of welding region.
3. Heat quantity depends on the variables of welding process (voltage, current, ..etc)
4. From the results of the microscopic structure it is evident that the geometric shape has an important role in the welding process. That is when the geometric value (15°V, 30°V and 45°V shape) of the welding region gets bigger, the faults get less due to increase of heat quantity in the welding region.
5. The work presents the finite element model for numerical simulation of welding stresses in low carbon steel St37 butt welding. The welding simulation was considered as a direct coupled thermo- mechanical analysis.
6. In the Butt welding region the corrosion rate for rain water is less than of sea water.

References

- [1] Abid Al-Razaq I.K, Nawfal Al-Aaragi and Ahmed A. Abar “Welding Technology“, 1993.
- [2] Medvedv,S.V. “Computer Modeling of Residual Welding Strains in Technological Design of Welded Structures”, Welding International., 2002, Vol.16,(1), pp. 59-65.
- [3] Hani A.A. “Finite Element Method for Thermo-Elasto Plastic Stress Analysis of Three Dimensional Problems” Ph.D. Thesis, Mech. Eng. Dept., Univ. of Tech. , 1998.
- [4] Lindgren LE, Haggblad H.A., Josefson B.L., Karlsson L. “Thermo – mechanical FE- Analysis of Residual Stresses and Stress Distribution in Butt Welding of Copper Canister of Spent Nuclear Fuel”, Eng. & Design, Vol. 212 , P.401-408, 2002.
- [5] Anas Yaghi and Adib Becker “Weld Simulation using Finite Element Methods”, report for Nottingham University , FENET-UNOTT-DLE-08, 2004.
- [6] Dragi Stamenkovic, Ivana Vasovic “Finite Element Analysis of Residual Stress in Butt Welding Two Similar Plates” Scientific Technical Review, Vol. LIX, No.1, 2009 .
- [7] Hani A. Ameen and Khairia S. Hassan "Influence of Butt Welding Shapes Design on the Microstructure and Stresses of Low Carbon Steel" , Eng.& Tech. Journal, Vol.28, No.15, 2010.
- [8] P.L. Cabot, F.Centllas, J.A Garrido “Influence of Heat Treatment in the Electrochemical Corrosion Al –Zn-Mg Alloys” Journal of Applied Electrochemistry. October 1991.
- [9] N.Birbilis, Z and R.G Buchheit “Electrochemical Characteristics of Intermetallics Phases in Aluminum Alloys an Experimental Survey and Discussion “Fontana Corrosion Center, Department of Materials Science and Engineering, 2005.
- [10] User’s manual of FEA/ANSYS/ Version 5.4 , 1997 .
- [11] Saeed Mouveni “Finite Element Analysis” , Theory and Application with ANSYS, Prentice Hall Press,1999.

Table(1) The Chemical properties of the used metal St 37

Wt% of element	C	Si	Mn	Cr	Mo	Cu	Co	V	W	Ai	Ni	P	S
Actual value %	0.2	0.009	0.65	0.011	0.004	0.041	0.004	0.0009	0.003	0.001	0.012	0.09	0.05
Standard value %	0.18-0.23	0.01	0.3-0.6	-	-	-	-	-	-	-	-	0.04	0.05

Table (2) Conditions of the welding process

	Current I (Amp)	Voltage V	Welding speed (S) m/min	No. of passes	Metal thickness mm	Input heat quantity (Joule)
15° angle	286	29.5	6	3	10	4.6x10 ⁷
30° angle	296	30.5	8.5	3	10	3.5x10 ⁷
45° angle	296	30.5	8.5	4	10	3.5x10 ⁷

Table (3) The Chemical composition of wire welding

element	C	Si	Mn	P	S	al	Ni	Cr	Cu	Mo
Wt%	0.068	0.763	1.41	0.02	0.014	0.002	0.041	0.026	0.026	0.002

Table (4) Material properties[6]

Temperature (°C)	Specific Heat (J/kg°C)	Conductivity (W/m°C)	Density (kg/m ³)	Yield Stress (MPa)	Thermal Expansion Coefficient (10 ⁻⁵ /°C)	Young's modulus (GPa)	Poisson's
0	480	60	7880	380	1.15	210	0.3
100	500	50	7880	340	1.2	200	0.3
200	520	45	7880	315	1.3	200	0.3
400	650	38	7760	230	1.42	170	0.3
600	750	30	7600	110	1.45	80	0.3
800	1000	25	7520	30	1.45	35	0.3
1000	1200	26	7390	25	1.45	20	0.3
1200	1400	28	7300	20	1.45	15	0.3
1400	1600	37	7250	18	1.45	10	0.3
1550	1700	37	7180	15	1.45	10	0.3

Table (5) Corrosion rate

Butt Angle	Specimen symbol	I [$\mu\text{A}/\text{cm}^2$]	V [mV]	Icorr. = 0.44*I
15°	A	22.7	620.1	9.988
	B	4	557.1	1.76
30°	A	56.9	615.3	25.036
	B	3.3	528.4	1.452
45°	A	64.4	639	28.336
	B	2.8	587.3	1.232

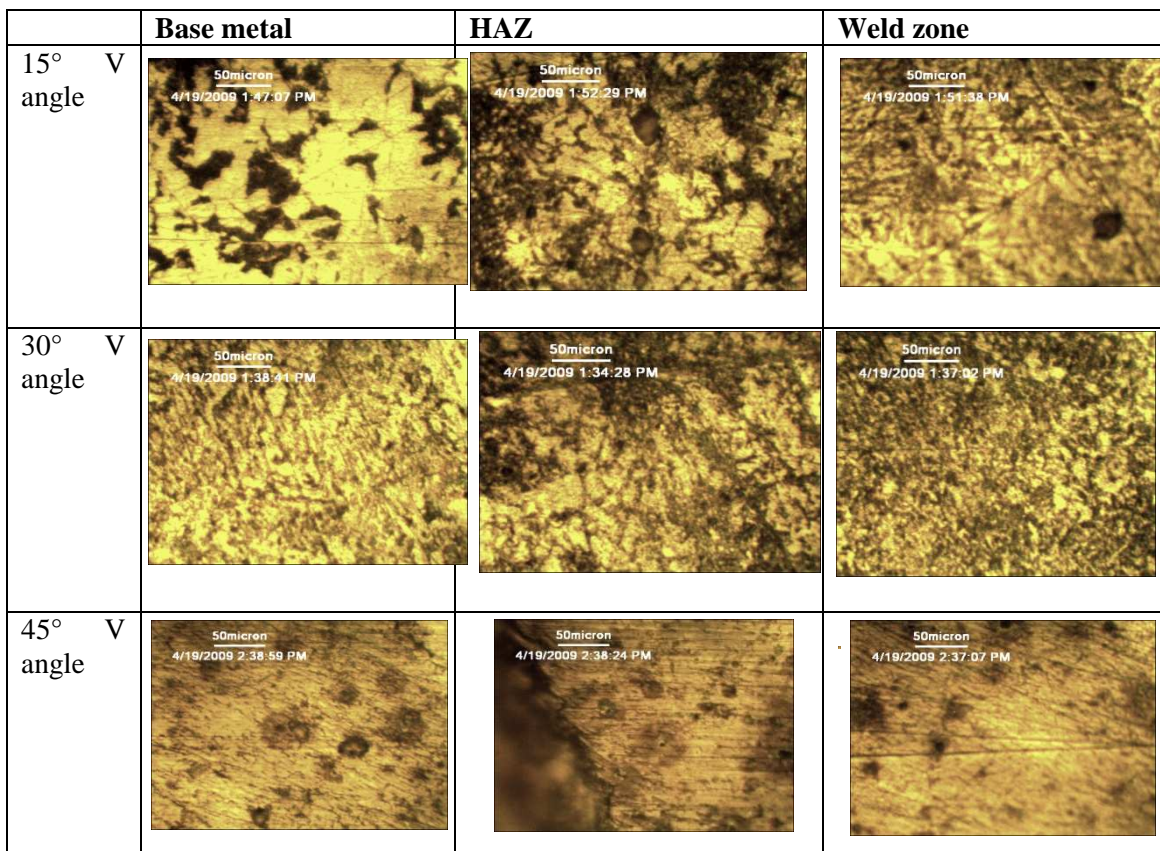


Figure (1) Show the microstructure of butt welding, it is clear from these plates there is no porosity according to X-ray radiography and the phases in these microstructure are ferrite -yellow places- and perrlite – black places- and the darkness places is cementite

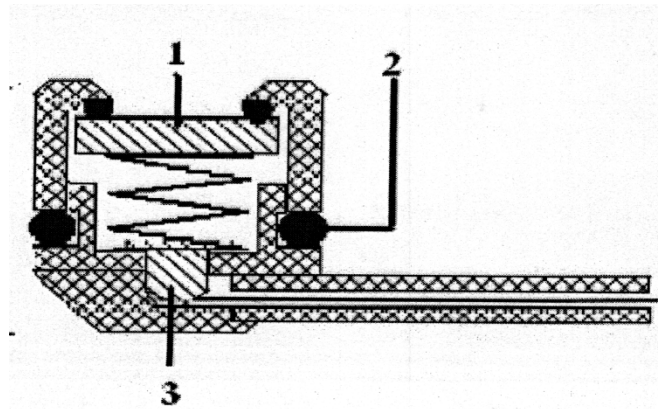


Figure (2) The specimen holder
1. Specimen 2. Seal 3. Electrical connection



Figure (3) Polarization standard cell

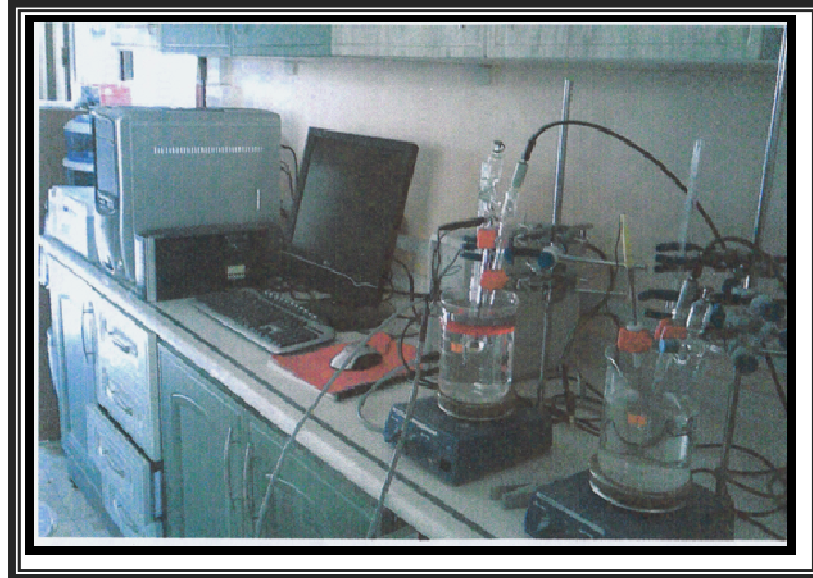
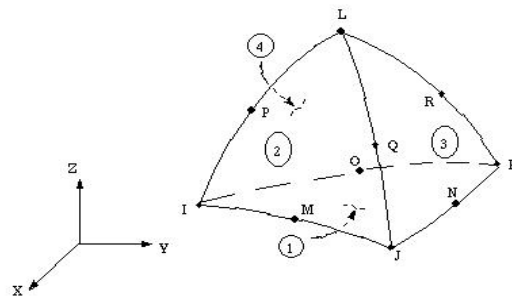


Figure (4) Potentiostat apparatus for polarization tests



SOLID98 Tetrahedral Coupled-Field Solid

Figure (5) Element type used in the analysis

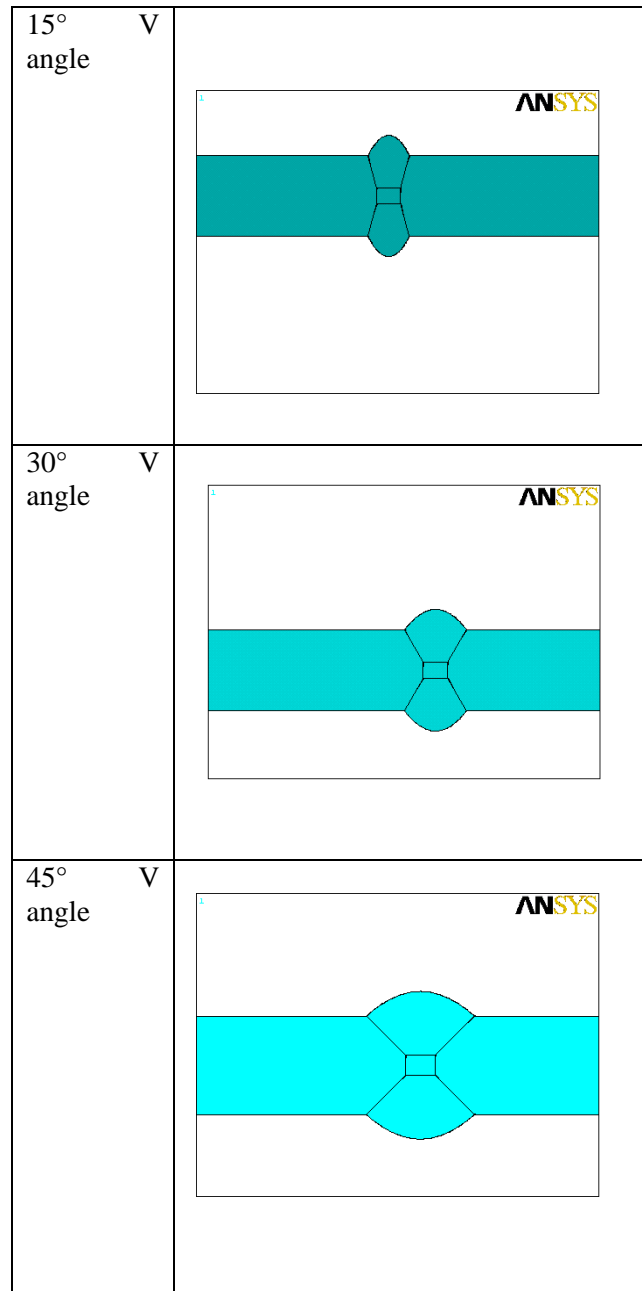
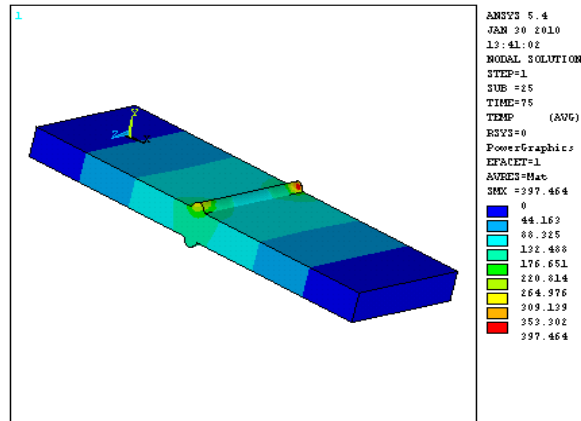
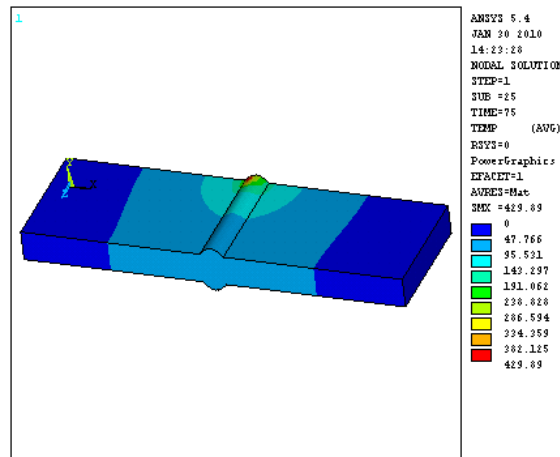


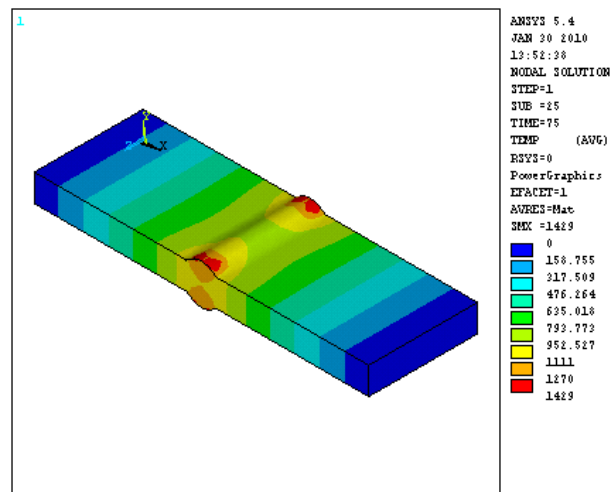
Figure (6) Models used in the analysis



Temperature Distribution V15°



Temperature Distribution V30°



Temperature Distribution V45°

Figure (7) Temperature distribution

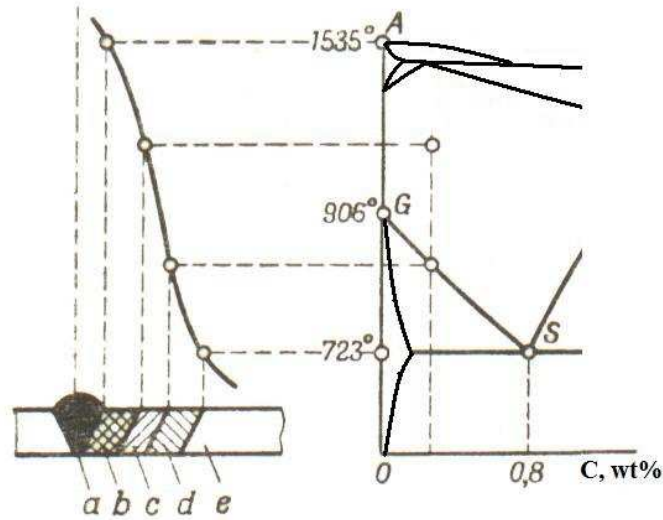


Figure (8) The structure of the welded piece (a- weld zone , b- heat effected zone, c- heated zone (Temp. above the GS line), d- heated zone (Temp. below the GS line) , e-base metal)

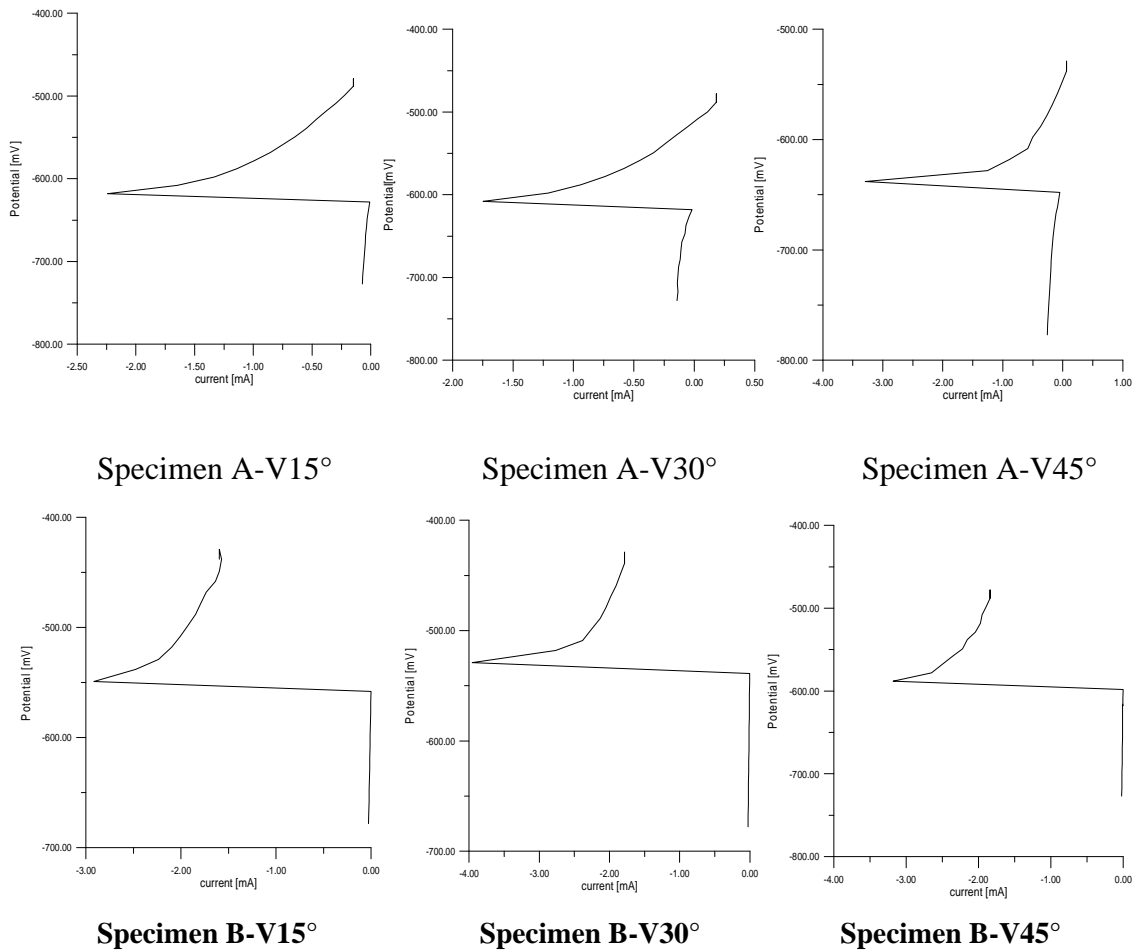


Figure (9) Tafel & cyclic polarization curve of low carbon steel in sea and rain water